

# Enhancement of the Inductive Operating Range of a TCSC in the High-Voltage Grid using a Mechanically Switched Series Reactor

T. Wenzel

T. Gaertner

T. Leibfried

Institute of Electric Energy Systems and High-Voltage Technology

Karlsruhe Institute of Technology, Germany

wenzel@kit.edu

thomas.gaertner@kit.edu

thomas.leibfried@kit.edu

**Abstract**—This Paper shows one of the possibilities to use Vacuum Circuit Breakers (VCBs) in flexible AC transmission systems in the High-Voltage Grid. A mechanically switched reactor, which is series connected to a TCSC in order to enhance the inductive working range is investigated. VCBs are used as switching elements as they can be switched more often without maintenance compared to other circuit breakers. Nevertheless, the switching frequency is strongly limited by their mechanical properties. In order to extend the application range to faster events like damping of power oscillations, more VCBs are switched in parallel to each other. Hence a higher periodically switching ability could be achieved. In this paper, it could be shown that the mechanically switched series reactor is able to enhance the damping of power oscillations. Furthermore the electrical stress on the VCBs and on the reactors for different simulation cases has been assessed. The simulation is performed with PSCAD.

**Index Terms**—Simulation, MSSR, TCSC, inductive range, PSCAD.

## I. INTRODUCTION

Usually Thyristor Controlled Series Capacitors (TCSCs) are used for power oscillation damping (POD) in extensive transmission systems. While damping a power oscillation, the TCSC runs mainly in the capacitive range because the thyristor currents reach undesired high values in the inductive range [1], [2], [3]. The idea is to enhance the inductive working range with a mechanically switched series reactor (MSSR) using Vacuum Circuit Breakers (VCBs) in a special configuration as switching elements. The reactor can be short-circuited by the VCBs.

Power oscillations may occur after disturbances in electrical power systems like line faults or station blackouts. Fig. 1 shows the transmittable power before, while and after a short-circuit in a transmission system over the load angle. The intercept point A at  $\delta_0$  marks the steady state operation point before the short-circuit. While the short-circuit occurs the demand of electrical power is lower than the turbine power so the rotor of a generator accelerates. The change of kinetic energy complies to area A1 [4]. Because of the high moment of inertia, this process can take up to some ms without loss of synchronism. After eliminating the short-circuit the demand of electrical power is higher than the turbine power because of larger load angle and hence the rotor decelerates.

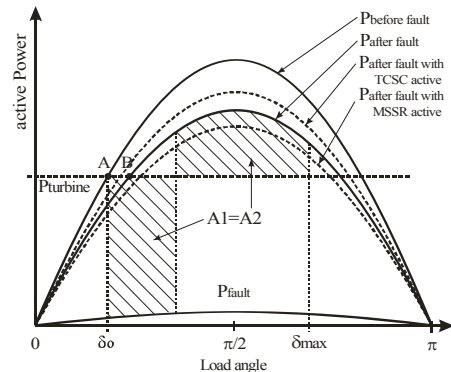


Fig. 1. Transmittable power over load angle

The maximum load angle is reached when the released kinetic energy is equal to the absorbed energy. The power curve after the fault has a smaller amplitude than the curve before the fault because of a line outage in the regarded case. The larger the decelerating area A2, the lower the maximum load angle will be. But at the point of maximum load angle, the rotor continues decelerating because the electrical power demand is still higher than the turbine power. This process continues into the other direction and the load angle oscillates around the new stationary point B until the oscillation has decayed. Generally, the power oscillation is damped by the damper windings of the synchronous generator and by power system stabilizers but in some cases, the damping is insufficient. Additional damping is then necessary in order to return into a stable operation point.

## II. SYSTEM DESIGN

### A. TCSC in combination with the MSSR

In order to damp a power oscillation the TCSC has to work in the maximum capacitive range directly after a fault in order to increase the decelerating area (see curve  $P_{\text{after fault with TCSC active}}$ ) until the maximum load angle  $\delta_{\text{max}}$  is reached. At this moment, the MSSR has to be inserted into the line and the capacitive reactance of the TCSC has to be minimized. This will lead to a lower maximum of the power curve (see curve  $P_{\text{after fault with MSSR active}}$ ), so the rotor will not go on decelerating that much as without MSSR. At the power minimum, the MSSR has to be removed again and the capacitive reactance of the TCSC has to be increased. This process can be repeated

until the power oscillation is damped sufficiently. The MSSR has to be inserted and removed again in every power swing period. Assuming that the oscillation frequency was 1 Hz, the MSSR had to be switched every 0.5 s. Therefore, it can be short-circuited by VCBs. In steady state of the power system, it remains short-circuited.

### B. Vacuum Circuit Breakers

VCBs are mainly available in the medium voltage range [5]. The VCBs used in this investigation have a rated voltage of 36 kV and a rated current of 2.5 kA [6]. Their rated short-duration power-frequency withstand voltage is 96 kV. This value is used as the maximum voltage capability of the VCB model. The tubes need maintenance after 30.000 switching operations, the mechanical parts after 10.000 switching operations [7]. Considering the expected number of switching operations and the voltage and current requirements, this type of breaker seems to be adequate. The VCB used in this investigation has a special operating mechanism and is assumed to be able to switch every second, so the following operating sequence is attainable: O-1s-C-1s-O-1s-C. One VCB of this kind is too slow to damp a power oscillation with a maximum frequency of 1 Hz, but with a combined series and parallel configuration according to Fig. 2, it is possible. Table I shows the switching status of the VCB configuration, in order to insert and to remove the reactor into the controlled line with a frequency of 1 Hz. In the first row is given the status of the reactor. The minimum time to the next status change of each VCB is 1.5 s as three cycles have to pass by. The final status after every damping process is the short-circuited reactor (status 0). It should be mentioned, that VCBs have an on- and off-delay time. The on-delay time is the time from closing command to closed contacts and the off-delay time from opening command to the start of movement of the contacts. In case of this investigation, both delay times are set to a constant value of 45 ms according to [7]. As this delay time is short compared to the period of one power swing a negative influence on the damping performance is not expected.

### C. Controller design

The controller design is based upon the residue method. Considering (1) the  $i$ -th eigenvalue  $\lambda_i = \sigma_i \pm j\omega_i$  of the state matrix can be calculated where the real part of the eigenvalue is the damping and the imaginary part is the frequency of the oscillation [8].

$$\begin{aligned} \Delta \dot{x} &= A\Delta x + B\Delta u \\ \Delta y &= C\Delta x \end{aligned} \quad (1)$$

Following matrices are introduced in order to express the eigenproperties of matrix A [8]:

$$\begin{aligned} A\Phi &= \Phi\Lambda \\ \Psi A &= \Lambda\Psi \\ \Psi &= \Phi^{-1} \end{aligned} \quad (2)$$

$\Lambda$  is the diagonal matrix of the eigenvalues.

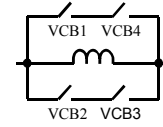


Fig. 2. VCB configuration for periodically switching

TABLE I  
SWITCHING STATUS OF THE VCB CONFIGURATION

Status	0	1	0	1	0	1	0	1	0
VCB1	C	O	O	O	C	C	C	C	C
VCB2	O	O	C	C	C	C	C	O	O
VCB3	C	C	C	O	O	O	C	C	C
VCB4	C	C	C	C	C	O	O	O	C

1: Reactor inserted / 0: reactor short-circuited

In order to modify an oscillation mode by feedback, the input must excite the mode and the change has to be identifiable in the output. The modal controllability and observability matrices are defined as following [9], [10]:

$$\begin{aligned} B' &= \Phi^{-1}B \\ C' &= C\Phi \end{aligned} \quad (3)$$

The matrix  $B'$  represents the controllability and  $C'$  the observability. The feedback between the output and input will only have an effect on the mode, if it is controllable and observable. For a Single Input, Single Output system the open loop transfer function of the system is described by (4).

$$G(s) = \frac{\Delta y(s)}{\Delta u(s)} = C(sI - A)^{-1}B \quad (4)$$

$G(s)$  can also be expressed in partial fractions of the Laplace transform of  $y$  as

$$G(S) = \sum_{i=1}^n \frac{R_i}{(s - \lambda_i)} \quad (5)$$

where the residue  $R_i$  of a mode indicates the sensitivity of the respective eigenvalue [11]. A system  $G(s)$  with a feedback control  $H(s)$  is shown in Fig. 3. If a feedback control  $H(s)$  is applied the real part of the eigenvalues of the original system  $G(s)$  are dislocated by  $\Delta\lambda_i = R_i H(\lambda_i)$  to the left half complex plane. A conventional lead-lag controller structure [12] is therefore used in this study. The transfer function of the controller consists of an amplification block, a wash-out block and  $n$  stages of lead-lag blocks.

$$H(s) = K \frac{sT_w}{1 + sT_w} \left[ \frac{1 + sT_{lead}}{1 + sT_{lag}} \right]^n = KH_1(s) \quad (6)$$

The washout constant  $T_w$  is usually in the range of 1-20 s.

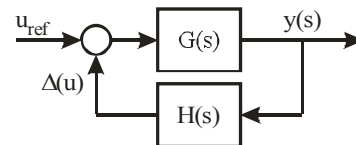


Fig. 3. Closed-loop system with feedback control

The lead-lag parameters can be determined using the following equations [8], [12]:

$$\begin{aligned} \varphi_{\text{comp}} &= 180^\circ - \arg(R_i) \\ a_c &= \frac{T_{\text{lead}}}{T_{\text{lag}}} = \frac{1 - \sin\left(\frac{\varphi_{\text{comp}}}{n}\right)}{1 + \sin\left(\frac{\varphi_{\text{comp}}}{n}\right)} \\ T_{\text{lag}} &= \frac{1}{\omega_i \sqrt{a_c}}, \quad T_{\text{lead}} = a_c T_{\text{lag}} \end{aligned} \quad (7)$$

$\arg(R_i)$  phase angle of the residue  $R_i$   
 $\omega_i$  frequency of the oscillation mode in rad/sec  
 $n$  number of compensation stages

One stage should not exceed  $60^\circ$  so  $n$  usually equals 2. The controller gain  $K$  can be calculated by (8) as a function of the desired eigenvalue location.

$$K = \left| \frac{\lambda_{i,\text{des}} - \lambda_i}{R_i H_i(\lambda_i)} \right| \quad (8)$$

The variable  $y(s)$ , see Fig. 3, is used as the POD controller input signal. Local signals like the active power, bus voltage or bus current are preferable [13], [10]. The active power was chosen as input signal because the residue ratio is in this case less sensitive on operating condition changes.

Regarding the investigated system the desired compensation phase angle is  $\varphi_{\text{comp}} = 77.5^\circ$ . Finally, the controller parameters are calculated as

$$H(s) = 30 \frac{s}{1+s} \frac{1+s0.083}{1+s0.306} \frac{1+s0.083}{1+s0.306}$$

The time delays of the firing control, the thyristors and the time delays of the VCBs are taken into account, too. For the TCSC, it is usually about 15-20 ms [12], and for the MSSR about 45 ms.

#### D. Protection of the reactor

In case of a short-circuit in the electrical network while the MSSR is inserted, the opened VCBs are stressed with high overvoltages as the high current flowing through the MSSR causes a high voltage drop. Hence a protective circuit has to be installed. A metal oxide varistor (MOV) switched into parallel to the reactor can serve this purpose. The MOV protects the device as soon as the maximum voltage is exceeded while the short-circuit current flows. The command to close the parallel VCB is directly given, as the short-circuit is detected. Once the short-circuit is removed, the VCB opens and the MSSR is utilizable for POD again. The MOV can meanwhile cool down. If the MSSR is short-circuited by the VCBs before a fault, which is the normal operating point, no problem is expected, because the VCBs can handle short-circuit currents up to 40 kA [7].

### III. SIMULATION MODEL

The simulation tool used is PSCAD, which is a graphical interface to the EMTDC software [14].

#### A. Electric network configuration

An electric network with a line-line voltage of 400 kV and a system frequency of 60 Hz is investigated in this study.

A generator is connected to a 400 kV-grid by three parallel transmission lines. Lines 1 and 2 have the same length of 125 km each. Line 3 represents a parallel corridor with a length of 150 km. The lines are modelled by a distributed RLC traveling wave model which is offered in PSCAD [14]. The used tower model is a Donau pylon [4]. Fig. 4 shows the electrical configuration.

The 400 kV-Grid is represented by a strong node with a short-circuit power of 100 GVA. The X/R-Ratio of the source impedance is 10. Therefore the impedance of this supply is  $X_s = 1.6 \Omega \cdot e^{j84.24^\circ}$ .

The synchronous generator symbol represents 4 machines with 700 MVA each. The rated voltage of every generator is 21 kV and the inertia constant is  $H = 5$  s. The inertia constant has a huge impact on the power oscillation frequency as well as the chosen voltage level, impedance of the transmission system, and stationary load angle before the fault [8]. To identify the undamped natural frequency the total system including the TCSC and the MSSR can be linearized by equation (1). With the classical model of the generator and all resistances neglected [8] the undamped frequency is calculated by (9).

$$\omega_n = \sqrt{\frac{E' E_B}{X_r} \cos \delta_0 \frac{\omega_0}{2H}} \quad (9)$$

For a Single Machine Infinite Bus (SISO) system there is one natural frequency. But a change in the grid configuration like an outage of a power line also causes a change in the frequency. The respective values are given in Table II.

The combination of TCSC and MSSR is inserted at station A as can be seen in Fig. 4. The degree of compensation of the TCSC is set to approximately 8% of line 1 and the inductance of the MSSR is 20 mH in the base scenario. The TCSC is working at lowest capacitive reactance in steady state which is  $3 \Omega$ . The TCSC capacitance is  $875 \mu\text{F}$  and the TCSC inductance is 1.26 mH. The maximum achievable capacitive reactance of the TCSC is three times the steady state value at a control angle of approximately  $148.4^\circ$ .

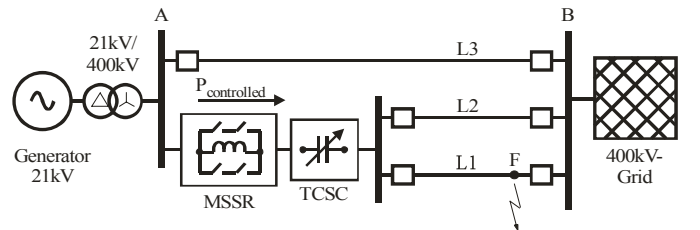


Fig. 4. Electric network configuration

TABLE II  
EIGENVALUES AND DAMPING RATIO

line outage	$\sigma$ ( $s^{-1}$ )	$\omega$ ( $rad \cdot s^{-1}$ )	$\zeta$
none	0.147	6.42	0.022
line 2	0.080	5.65	0.014
line 3	0.106	5.95	0.018

The MSSR has a reactance of  $7.5 \Omega$  reduced to  $4.5 \Omega$  by the reactance of the TCSC in steady state. The quality factor of the MSSR inductance is set to 180 so a series resistor with  $42 \text{ m}\Omega$  is considered in every phase.

In the base scenario, the generator transmits 2255 MW into the grid. Line 1 and 2 are loaded by 834 MW each and line 3 by 587 MW. The maximum current of the MSSR is limited to 2.5 kA due to the ratings of the VCBs. In the base scenario the current through the MSSR is 2.43 kA. A fault can be applied at point F. All simulated cases together with further parameters are mentioned in section simulation results.

### B. VCB configuration

The VCB model used in this investigation has been described in [15] where it was used to simulate a vacuum contactor. However, it can be used for modelling a VCB with new parameters, which are given in Table III. The maximum voltage of the considered VCB is taken from data sheet [7]. The arc voltage is within the range of 20 V to 30 V [5] and can be neglected in case of this investigation. It is only required if energy conversion in the tube has to be considered. The chopping current is set to a constant value of 5A differing from [15]: The simulation results are then comparable and it represents the worst case scenario, as typical values of VCBs lie in the range of 2 A – 5 A [5], [6]. The value of the dielectric recovery slope is estimated.

## IV. SIMULATION RESULTS

PSCAD calculates the differential equation solutions of the electrical system with a constant step size. The stepsize for all simulations was set to  $10 \mu s$ . If a different step size has been used, it is mentioned in the respective part of this paper.

The time until an occurring power oscillation has decayed is assessed for three different cases in the first scenario: 1) the MSSR and the TCSC are both in service, 2) only the TCSC is in service and 3) no additional damping is delivered. The results are shown in Fig. 5. A grounded three phase fault is applied at point F (Fig. 4), and after 80 ms it is removed by tripping line 2. The active power in line 1 after the fault is 1274 MW.

TABLE III  
SETUP PARAMETERS FOR THE VCB MODEL

Parameter	Value
maximum voltage	96 kV
Resistance (open)	$1000e6 \Omega$
Resistance (closed)	$80e-6 \Omega$
slope of dielectric strength	5 kV/ $\mu s$
slope of dielectric recovery	15 kV/ms

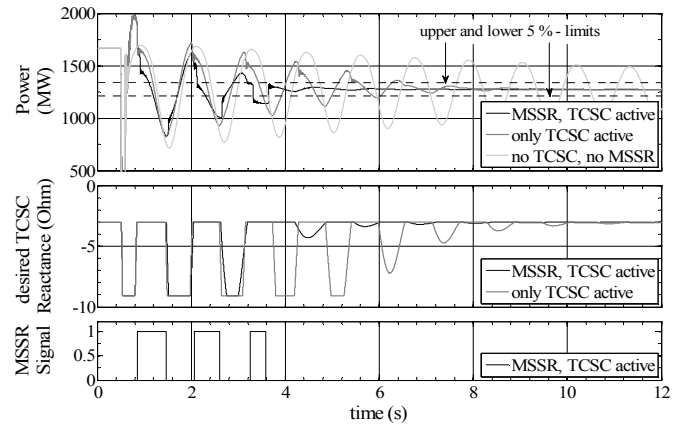


Fig. 5. Damping of the power oscillation:  $L_{MSSR} = 20 \text{ mH}$ ,  $C_{TCSC} = 875 \mu F$ ,  $L_{TCSC} = 1.26 \text{ mH}$ ,  $X_{TCSC} = 3 \dots 9 \Omega$ ,  $X_{MSSR} = 7.5 \Omega/0 \Omega$

The upper graph shows the transmitted active power  $P_{controlled}$ . The upper and lower 5% - limits are given by the dashed lines. The middle graph shows the desired reactance of the TCSC, which is limited to the capacitive range. Every time a threshold value of the desired reactance is exceeded, the MSSR is activated. The lower graph shows the switching command of the MSSR. It can be seen in the upper graph that the power oscillation decays much faster if both – the TCSC and the MSSR – are in service. The peak-peak amplitude of the oscillation gets within the 5% - limits after 27 s without additional damping. If only the TCSC is active the oscillation needs approximately 6 s to get into the 5% range. If both elements are active, it takes only 3 s. In this example the reactor has been inserted into the line three times. It takes nearly half of the time until the oscillation has died out.

### A. Influence of the MSSR reactance on POD

Fig. 6 shows the damping of the power oscillation for three different impedances of the inserted MSSR in the base scenario: 10 mH, 20 mH, and 30 mH. If the inductance is 10 mH the additional damping is not sufficient and the VCBs have to be switched very often. The oscillation needs at least 4.2 s to get into the 5% - limits. The situation is improved considerably by choosing an inductance of 30 mH. Now the 5% - limits are reached within 2.5 s and there are only two switching operations. But this inductance value is too high if the power oscillation amplitude is lower. This can be the case if other fault types or shorter fault durations occur.

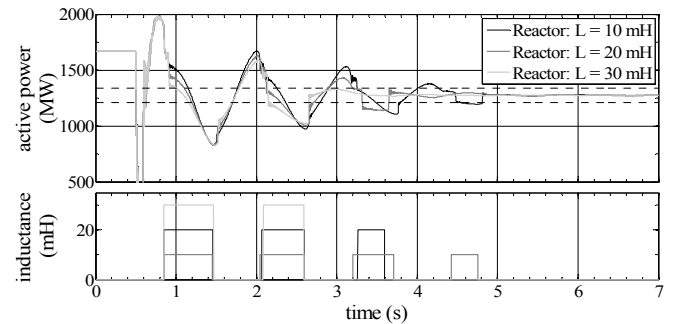


Fig. 6. POD for different MSSR reactances

It was figured out within this investigation, that the MSSR with 30 mH could not be inserted in many of such simulated cases, because it would have had a negative influence on the power oscillation damping performance. A compromise between an enhanced operative range and a sufficient damping is reached by an inductance of 20 mH, according to the base scenario, which is 20.5 % of the line inductance. There are now 3 switching operations and the 5 % - limit is reached within 3 s.

### B. POD for different fault types and times

Table IV gives an overview over the times needed so that a power oscillation gets within the 5 % - limits for different fault durations and line outages with and without the MSSR. The fault type changes only the amplitude of the power oscillation and has therefore the same effect as the fault duration, so a 3 phase grounded fault is always assumed. In case of an outage in line 3, the fault is applied directly to the right terminal of this line, see Fig. 4. The POD takes always less time, if the MSSR is utilized. Only in case 5 the MSSR cannot improve the POD because the fault produces only a small power amplitude. It should be mentioned that in cases 2 and 5 the MSSR is overloaded by 30 % after line 3 outage. That is no problem for approximately 10 min because the considered VCBs are able to carry 1.5 times their rated current which is 3.75 kA within this time. If it takes longer to reconfigure the electrical network the transmitted power has to be reduced.

In the following sections is assessed the electrical stress on the components of the MSSR for the base scenario.

### C. Currents and Voltages of VCBs and Reactor

A current of 2.43 kA flows through the two VCBs which are short-circuiting the reactor in steady state operation before the fault occurs. If one of them is opened, the current is shifted to the reactor. This can be seen in the lowest graph of Fig. 7. Every time the reactor is short-circuited again, a DC-Trapped current occurs, which decays with a time constant of  $\tau = R_{MSSR}/L_{MSSR} = 0.48$  s. When the respective VCB opens the first time, the maximum voltage across it reaches a value of 31 kV in phase s which is far from the maximum rating of the VCB. Fig. 8 shows the detailed Transient Recovery Voltage (TRV) across the opening VCB when the MSSR is inserted the first time as well as the dielectric recovery of the gap. The simulation stepsize was in this case set to 1  $\mu$ s.

TABLE IV  
POD TIMES FOR DIFFERENT FAULT DURATIONS AND LINE OUTAGES

No.	fault time in ms	line outage	Power after fault in MW	Power amplitude in MW	POD time with MSSR in s	No. of switchings	POD time without MSSR in s
1	80	L2	1274	1988	<b>3.1</b>	3	6.0
2	80	L3	2255	3916	<b>0.9</b>	1	1.9
3	80	none	1667	3438	<b>1.7</b>	2	3.1
4	40	L2	1274	1741	<b>2.1</b>	2	3.6
5	40	L3	2255	3145	<b>1.3</b>	1	1.1
6	40	none	1667	2663	<b>1.1</b>	1	2.1

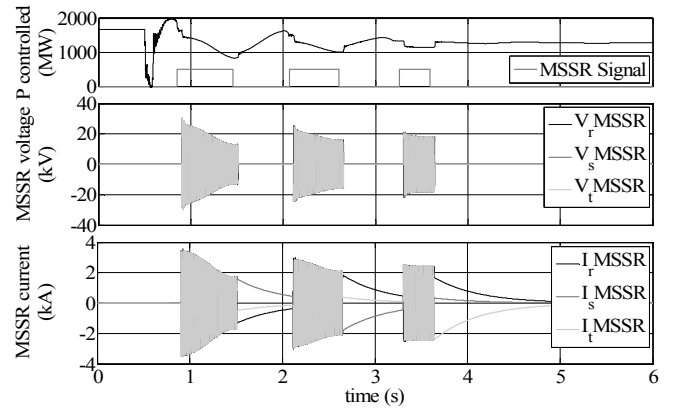


Fig. 7. Currents and voltages of the MSSR

At  $t = 0.007$  s the contacts are starting to open and the recovery voltage is increasing. As current through VCB falls below the value of chopping current, it is interrupted immediately and a TRV occurs. The first peak at  $t = 0.008$  s is an unsuccessful interruption. The TRV exceeds the dielectric strength of the opening gap and a restrike occurs. Current goes on flowing until next zero crossing and is then successfully interrupted at  $t = 0.017$  s. The peak value and frequency of the oscillation of the TRV depend on the inductance and the line capacitances to ground. The TRV slope is in this case approximately  $0.3$  kV/ $\mu$ s and within the range of VCB parameter of  $5$  kV/ $\mu$ s. It should be mentioned, that the moment of MSSR insertion does not change the maximum amplitude of the TRV but indirectly it changes the starting position of the recovery voltage ramp and therefore the height of the first small peak. The TRV peak value is affected by the short-circuit duration: The amplitude of power oscillation increases and so does the current through the controlled line. The maximum inductance value of a reactor has to be adapted to the maximum current which can occur during a power oscillation, because it affects the voltage drop across the reactor. This depends on the regarded electrical network and the fault types which are expected in it.

### D. Two MSSRs

If for any reason a finer gradation of the MSSR impedance is desired one fact has to be considered, which is described in this section. Assumed that two MSSRs are utilized each with half of the original reactance, the stray capacitances of the MSSR can have a negative effect on the switching capability of the VCBs. To investigate this effect, a stray capacitance of 50 pF is added between both MSSRs to ground.

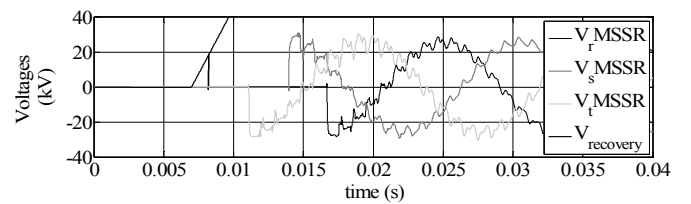


Fig. 8. Detailed TRV across the opening VCB

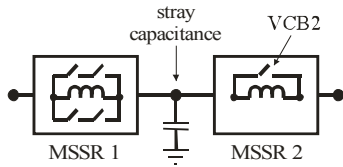


Fig. 9. Stray capacitance between the MSSRs

The stray capacitances at both terminals which are directly connected to the lines are neglected because they are very small compared to the line capacitances.

If there is a need for a high inductive reactance both MSSRs have to be inserted into the line. The insertion of the first MSSR will take place without problems as mentioned in section IV.C. But if after a short time the second MSSR is inserted, which means that VCB2 in Fig. 9 has to be opened, the arising TRV peak is mainly affected by the stray capacitance and the inductance of the switched MSSR. The TRV can have a very high peak with a high slope. This worst case scenario is shown in the upper graph of Fig. 10. Although the maximum voltage of the VCB is not exceeded, a current interruption is impossible because the slope of the TRV is about  $27 \text{ kV}/\mu\text{s}$ , much higher than what the VCB is able to handle. This leads to restrikes in the VCB in all phases, which can be seen when there are spikes at the moment of the current zero crossings in every phase. The current cannot be successfully interrupted. A possibility to avoid transients at the VCBs with high amplitudes and large slopes is to connect a capacitor with higher value compared to the stray capacitance parallel to it. This effect can be seen in the lower graph. The capacitance across the VCB was in this case set to  $600 \text{ pF}$  and the situation is enhanced considerably. The slope is  $4.31 \text{ kV}/\mu\text{s}$  and the amplitude is  $25 \text{ kV}$  both within the VCB parameters. The frequency of the oscillation is approximately  $63 \text{ kHz}$ . No additional capacitor is necessary, if the stray capacitance has a minimum value of  $500 \text{ pF}$ . In real configuration, the stray capacitance of the reactor has to be well estimated. If problems are expected, an additional parallel capacitor should be provided for the VCBs due to protective reasons.

## V. CONCLUSION

This paper shows that a mechanically switched tapped reactor can support a TCSC in order to maintain a better performance for power oscillation damping by enhancing the inductive range of the TCSC.

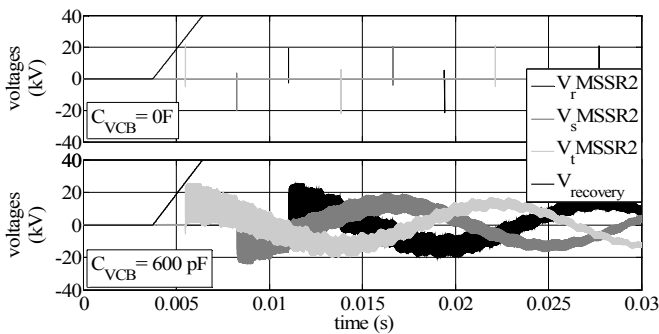


Fig. 10. Detailed TRV across the opening VCB

The time until the power oscillation reaches a satisfactory value could be reduced up to half of the time in the investigated cases. The resulting electrical stress on the components like the reactor and the VCBs while switching operations occur does not exceed the parameter of the used VCBs. It was found out in this investigation that a reactor impedance of approximately  $7.5 \Omega$  leads to an optimal damping process for the considered configuration because it delivers sufficient damping and only few switching operations are necessary.

If two MSSRs are utilized, the stray capacitance has a big influence on the TRV if one MSSR is already inserted into the line and the second should be inserted. High TRV peaks and slopes can occur across the opening VCB. If they exceed the limits of the VCB parameters, a capacitor connected in parallel to the respective MSSR improves the situation considerably.

The actual POD controller will be enhanced by an adaptive phase-compensation control based on prony analyses or Kalman filter for frequency identification. Additionally, a nonlinear controller for POD will be introduced. It is furthermore intended to extend the controller in order to operate in more complex network configurations.

## REFERENCES

- [1] E. V. Larsen et al., *Characteristics and rating considerations of thyristor controlled series compensation*, IEEE Transactions on Power Delivery, vol. 9, pp. 992–1000, April 1994
- [2] Y. H. Song, A. T. Johns, "Flexible ac transmission systems (FACTS)", The Institution of Electrical Engineers, London, United Kingdom, 1999
- [3] R. M. Mathur, R. K. Varma, "Thyristor-Based FACTS Controllers For Electrical Transmission Systems", Institute of Electrical and Electronics Engineers, Inc., United States of America, 2002
- [4] D. Oeding, B. R. Oswald, "Elektrische Kraftwerke und Netze", 6th ed., Springer-Verlag, Berlin Heidelberg, New York, 2004
- [5] H. J. Lippmann, *Schalten im Vakuum – Physik und Technik der Vakuum-Schalter*, Berlin, Offenbach, VDE-Verlag GmbH, 2003
- [6] Siemens, "Vakuum-Schalttechnik fuer die Mittelspannung", Katalog HG 11.01, 2007
- [7] Siemens, "Vakuum-Leistungsschalter 3AH2/ 3AH4", Katalog HG 11.04, 2007
- [8] P. Kundur, "Power System Stability and Control", McGraw-Hill inc., United States of America, 1994
- [9] M.W. Mustafa, N. Magaji, "Optimal Location of Static Var Compensator Device for Damping Oscillations", American J. of Engineering and Applied Science 2, 2009
- [10] A. Feliachi, L. Fan, K. Schoder, "Selection and design of a TCSC control signal in damping power system inter-area oscillations for multiple operating conditions", Electric Power Systems Research 62, 2002
- [11] J. D. McCally et al., "TCSC Controller Design for Damping Interarea Oscillation", IEEE Transaction on Power Systems, Vol. 13, No. 2 November 1998
- [12] Z.Xu, Y.F.Lin, Y.Huang, "Power Oscillation Damping Controller Design for TCSC Based on The Test Signal Method", Power Engineering Society General Meeting, IEEE, 2005
- [13] A. D. Del Rossom, A. Cañizares, V.M. Doña, "A Study of TCSC Controller Design for Power System Stability Improvement", IEEE Transaction on Power Systems, February 2003
- [14] "PSCAD Electromagnetic Transients – User's Guide", Manitoba HVDC Research Centre Inc., 2005
- [15] T. Wenzel, T. Leibfried, D. Retzmann, "Dynamical simulation of a Vacuum Switch with PSCAD", 16th Power Systems Computation Conference, Glasgow, Scotland, 2008